Czech Phycological Society

Fottea, 26(1), 94–106, 2026
doi: 10.5507/fot.2025.018

Morphology and molecular phylogeny of phylogroup *Characiosiphonia* (Chlamydomonadales, Chlorophyceae), with the description of a new species *Characiochloris papillata sp. nov.*

Qingyu Dai[1,2], Yangliang Chen[1,2], Huan Zhu[1], Benwen Liu[1] and Guoxiang Liu[1]

Abstract

The genera *Lobocharacium* Kugrens, Clay *et* Aguiar, *Characiosiphon* Iyengar, and *Characiochloris* Pascher form a distinct phylogenetic clade within the order Chlamydomonadales, here referred to as the *Characiosiphonia* clade. These taxa share a similar overall cell morphology, characterized by a narrowed apex and a basal attachment structure. However, these genera also exhibit different characters, and previous studies have not provided a comparative morphological analysis to distinguish among the three genera within this clade. In this study, we conducted detailed morphological and molecular investigations of four algal strains. Phylogenetic analyses based on 18S rDNA and *rbcL* sequences confirmed the position of the three genera within the *Characiosiphonia* clade. The molecular analyses indicate that the genus *Characiochloris* is not monophyletic. Based on its unique features and the irregular contractile vacuoles in cells, we describe the strain – FACHB–3671 as a new species and named it *Characiochloris papillata sp. nov.* Given the current limitations in the molecular data of *Characiochloris* Pascher (particularly the lack of its type species), further research is necessary to resolve its polyphyly and clarify the taxonomic boundaries of the *Characiosiphonia* clade.

Keywords

Characiosiphonia; Chlamydomonadales; Morphology; New species; Phylogeny; Taxonomy

[1] *Key Laboratory of Algal Biology, Institute of Hydrobiology, Chinese Academy of Sciences, Wuhan, 430072, China*
[2] *College of Advanced Agricultural Sciences, University of Chinese Academy of Sciences, Beijing, 100039, China*

Corresponding author
Guoxiang Liu
liugx@ihb.ac.cn

Article History
Received April 16, 2025
Revised November 27, 2025
Accepted December 8, 2025
Published online April 1, 2026

Supplementary Material
Available online

How to cite
Dai, Q., Chen, Y., Zhu, H., Liu, B., & Liu, G. (2026). Morphology and molecular phylogeny of phylogroup *Characiosiphonia* (Chlamydomonadales, Chlorophyceae), with the description of a new species *Characiochloris papillata* sp. nov. *Fottea*, *26*(1), 94–106. https://doi.org/10.5507/fot.2025.018

Introduction

The genus *Characiosiphon* Iyengar was established based on the type species *Characiosiphon rivularis* M.O.P. Iyengar and assigned to the family *Characiosiphonaceae* (Iyengar, 1936). The distinct morphology of *Characiosiphon* Iyengar, characterized by considerable variation in length, width, and the number and shape of its protoplasts, sets it apart from other genera (Sarma & Keshri, 1992). Moreover, based on its morphological and physiological traits, *Characiosiphon* was initially considered to be closely related to *Characium A. Braun* (Iyengar, 1936; Kützing, 1849). Bourrelly (1959) reclassified *Characiosiphon* within the family Chlorangiaceae of Tetrasporales. Fott (1959, 1972a) concurred with this order–level taxonomic position, but emphasized the distinctness and independence of both *Characiosiphon* and its family Characiosiphonaceae. The genus *Lobocharacium* was established with the type species *Lobocharacium coloradoense* P.Kugrens, B.L.Clay *et* R.Aguiar (Kugrens *et al.*, 2000) They described several key similarities and differences between *Lobocharacium* and *Characiosiphon*. Both cells are usually relatively large, fusiform, and multinucleate. They reproduce via zoospores. However, they can be readily distinguished based on their internal structures. For *Characiosiphon*, the vesicular thallus is filled with sap. Protoplasts of the uppermost part are compactly arranged, angular, pentagonal to hexagonal in surface view. The chloroplasts are stellate in young

© Czech Phycological Society (2026)

cells and diffuse in aging cells, making it difficult to recognize their shape. In contrast, the cytoplasm of *Lobocharacium* is divided into lobes interconnected by thin cytoplasmic bridges, each lobe bearing a single stellate chloroplast with a central pyrenoid, with numerous such chloroplasts present throughout the cell. The structural and reproductive features of *Lobocharacium* are more similar to *Characiosiphon* than *Characium*. Therefore, it was placed in the family Characiosiphonaceae (Kugrens *et al.*, 2000).

Since *Characiochloris* was first established by Pascher (1927), a total of 20 species have been described (Ettl & Gärtner, 1988; Fott, 1972b; Iyengar, 1975; Korshikov, 1953; Lee & Bold, 1974; Nozaki, 1993; Pascher, 1927; Proshkina, 1941; Skuja, 1948, 1956). The vegetative cells of *Characiochloris* are remarkably *Characium*–like, without a stalk and attached with a pad which may be encrusted with iron compounds (Lee & Bold, 1974). The cells are uninucleate and contain a single pyrenoid. Numerous small contractile vacuoles are randomly distributed within the cytoplasm and can be observed through the fissures of the chloroplast. The taxon produces biflagellate zoospores characterized by small contractile vacuoles, a parietal chloroplast, and an anterior nucleus. Adhesion is achieved through the flagella, which subsequently disappear. (Ettl & Gärtner, 1988; Fott, 1972a, b; Korshikov, 1953; Lee & Bold, 1974). Based on these morphological characteristics, *Characiochloris* has traditionally been classified within either Tetrasporales (Fott, 1972a, b; Lee & Bold, 1974) or Chlorococcales (Ettl & Gärtner, 1988). However, phylogenetic evidence has confirmed its taxonomic position within Chlamydomonadales (Buchheim *et al.*, 2002).

Characiosiphon and *Lobocharacium* were classified as the members of Characiosiphonaceae based on morphology. The taxonomic position of *Characiochloris* has been continuously changing with further research. Phylogenetic analyses have provided robust evidence supporting their classification and three genera formed a distinct lineage (i.e. *Lobocharacium* lineage, Buchheim *et al.*, 2002). Based on additional molecular data, the phylogenetic analysis conducted by Nakada *et al.* (2008) also confirmed this conclusion and named it the *Characiosiphonia* clade. This study provides a detailed description of the morphological characteristics of four algal strains. Phylogenetic analyses using the 18S rDNA and *rbcL* datasets confirm that these three genera belong to the *Characiosiphonia* clade. Moreover, we identified and formally described a novel species.

Material and Methods

Isolation of algae and establishment of cultures: The sampling information for the four newly obtained algal strains is presented in Table 1. Some collected samples were fixed in 4% formaldehyde solution for morphological observations, while others were used for single–colony isolation and culture. The strains were deposited in the Freshwater Algal Herbarium (IHB), Institute of Hydrobiology, Wuhan, China. For algal inoculation, cultures were grown on Bolds Basal. (BBM; Bischoff & Bold, 1963) supplemented with 1.5–2% agar in 6 cm diameter plastic Petri dishes. The cultures were incubated in a HP250G–C growth chamber (Ruihua Corp., Wuhan, China) under white fluorescent light at an irradiance of 30–50 µmol photons·m^{-2}·s^{-1}, with a 14:10 h light–dark photoperiod at a constant temperature of 22 °*C. S*ingle algal colonies were successively isolated and transferred to fresh BBM medium. Once colonies exhibited robust growth, they were transferred into liquid BBM for further cultivation. After one week of incubation, a small volume of the liquid culture was sampled and examined under a light microscope (Olympus BX53, Olympus Corp., Tokyo, Japan) for morphological characterization and imaging. Key morphological features were carefully observed, measured, and documented. Optical micrographs were captured using an Olympus DP80 camera (Olympus Corp., Tokyo, Japan) mounted on the microscope. Particular emphasis was placed on the detailed recording and photographic documentation of diagnostic taxonomic traits to ensure a comprehensive and precise taxonomic analysis.

DNA extraction and PCR amplification: Total genomic DNA was extracted using a commercial universal DNA isolation kit. Pure algal strains were harvested and transferred into 2 mL cryopreservation tubes, washed multiple times with phosphate–buffered saline (PBS, pH 7.2), and mixed with 0.5 mm diameter glass beads. Cell disruption was performed using a

Table 1. Sampling information and GenBank accession numbers newly obtained in this study.

Species	Strain	Habitat	Location	Date	GenBank accession numbers	
					18S rDNA	*rbcL*
*Lobocharacium coloradoen*se	FACHB–3670	Attached to *Oedogonium* sp.	Wuhan Hubei, China	May 20, 2022	PQ890287	PV005831
Characiosiphon rivularis	MTGZ01	Attached to sand	Wuhan Hubei, China	Sep 26, 2015	PQ890285	PV005832
Characiosiphon rivularis	WHGZ02	Attached to sand	Wuhan Hubei, China	Sep 26, 2015	PQ890286	PV005833
Characiochloris papillata	FACHB–3671	Attached to stones	Xuanwei Yunnan, China	Oct 10, 2022	PQ890284	PV005830

Fottea, 26(1), 94–106, 2026
doi: 10.5507/fot.2025.018

MiniBeadBeater bead mill tissue grinder (3110BX, Biospec Products, Bartlesville, Oklahoma, USA). DNA extraction followed the manufacturer's protocol of the AxyPrep MAG Plant Genomic DNA Extraction Kit (Corning Inc., Corning, New York, USA). PCR amplification was conducted in a 50 μL reaction mixture containing 5 μL of template DNA (25 ng·μL^{-1}), 25 μL of 2× Taq Master Mix (ExTaq, Takara, Dalian, China), 1.5 μL (10 μM) of each forward and reverse primer, and sterile deionized water to a final volume of 50 μL. Nuclear–encoded 18S rDNA sequences were amplified using the primers 18S–FA (5′–AACCTGGTTGATCCTGCCAG–3′) and 18S–RB (5′–TGATCCTTCTGCAGGTTCACCTA–3′; Nakazawa & Nozaki, 2004). The amplification conditions were as follows: initial denaturation at 94 °C for 5 min, followed by 35 cycles of denaturation at 94 °C for 50 s, annealing at 55 °C for 60 s, and extension at 72 °C for 90 s, with a final extension at 72 °C for 10 min. The *rbcL* gene was amplified using the primers *rbcL*–F (5′–ATGGTTCCACAAACAGAAAC–3′) and *rbcL*–R (5′–TTGTCATAGTATCAAATTC–3′; Nozaki *et al.*, 1995). The PCR protocol consisted of an initial denaturation at 94 °C for 2 min, followed by 2 min at 46 °C and 3 min at 66 °C, then 29 cycles of 94 °C for 1.5 min, 46 °C for 2 min, and 66 °C for 3 min, with a final extension at 72 °C for 15 min. All PCR amplifications were performed using a T100™ thermal cycler (Bio–Rad Corp., Singapore). PCR products were purified using the FastPure Gel DNA Extraction Mini Kit (Vazyme, Nanjing, Jiangsu, China) and sequenced with an ABI 3730xl DNA sequencer (Applied Biosystems, Foster City, California, USA) using the same primers. Newly obtained sequences were submitted to GenBank.

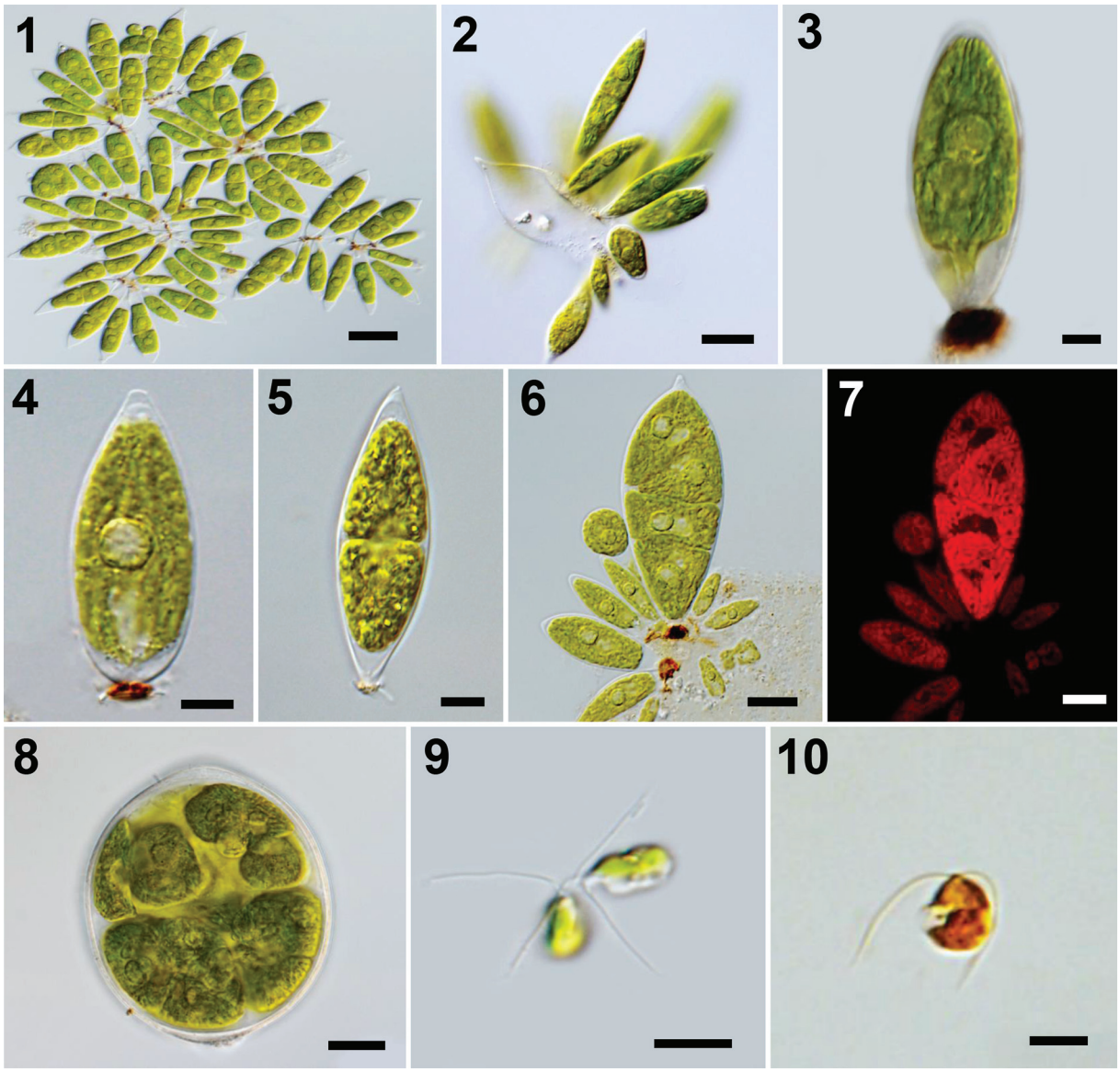
Phylogenetic analyses: All newly generated algal sequences from this study have been deposited in GenBank, with the corresponding accession numbers listed in Table 1. Additional sequences relevant to the phylogenetic analyses were retrieved from GenBank (http://www.ncbi.nlm.nih.gov).Given that the taxa examined in this study primarily belong to the order Chlamydomonadales, the 18S rDNA and *rbcL* datasets were selected to represent the major clades within Chlamydomonadales (Nakada et al., 2008). In total, 67 sequences were used for the construction of the 18S rDNA phylogenetic tree, including 63 sequences obtained from GenBank and 4 newly generated sequences from this study (Table S1). A total of 45 algal sequences were used to construct the *rbcL* phylogenetic tree, including 41 sequences retrieved from GenBank and 4 newly generated sequences from this study (Table S2). Sequence alignment was conducted using MAFFT v7.3 (Katoh & Standley, 2013) for 18S rDNA sequences, followed by manual refinement. For *rbcL* sequences, additional alignment was performed using the MUSCLE algorithm within MEGA11 with the "align codons" option enabled (Edgar, 2004; Kumar *et al.*, 2016), and manual adjustments were applied in MEGA11 (Tamura *et al.*, 2021). Phylogenetic trees were inferred using both Maximum Likelihood (ML) and Bayesian Inference (BI) methods, implemented in IQ–TREE2 (Minh et al., 2020) and MrBayes v3.2.7 (Ronquist *et al.*, 2012), respectively. The best–fit nucleotide substitution models were determined using ModelFinder (Kalyaanamoorthy *et al.*, 2017). For ML analysis, TN+F+I+G4 and GTR+F+I+G4 were identified as the optimal models for the 18S rDNA and *rbcL* datasets, respectively. Branch support was assessed using 1000 bootstrap (BP) replicates and the Shimodaira–Hasegawa–like approximate likelihood ratio test (SH–aLRT; Guindon *et al.*, 2010) with 1000 replicates. In BI analysis, SYM+I+G4 and GTR+F+G4 were selected as the most appropriate models for the 18S rDNA and *rbcL* datasets. The Markov Chain Monte Carlo (MCMC) analysis was conducted with two independent runs, each consisting of four chains (three heated and one cold), for a total of 2,000,000 generations. Trees were sampled every 1000 generations, with the first 25% discarded as burn–in. Convergence was confirmed when the average standard deviation of split frequencies dropped below 0.01. In this study, branches with maximum likelihood bootstrap (BP) values >80, Shimodaira–Hasegawa–like approximate likelihood ratio (SH–aLRT) values above 80% or Bayesian posterior probabilities (PP) >0.9 were considered significantly supported. When all were satisfied, the branches were regarded as strongly supported.

Results

Morphological observations

The strain FACHB–3670 grows outward in a circular pattern when forming colonies. At the base of the cells, a brown attachment pad connects cells or attaches other substrates (Fig. 1). Mature vegetative cells are large and spindle–shaped, with sharply tapered tips forming points or papilla. The widest region is at the middle, gradually narrowing towards the base (Fig. 2). Cells measure 30–90 μm in length and 10–25 μm in width. A prominent central pyrenoid is present (Figs 3, 4). From the cell surface, a lamellar chloroplast can be observed, and multiple cytoplasmic lobes interconnect via thin cytoplasmic bridges (Figs 6, 7). As the vegetative cells mature, each cytoplasmic lobe undergoes division, producing numerous zoospores (Figs 5, 8). Zoospores are oval or spindle–shaped, measuring 4–10 μm in length and 2–5 μm in width. They contain a single peripheral chloroplast with an eyespot and two equal–length flagella, the latter measuring approximately 1.5 times the length of the cell (Figs 9, 10). Zoospores are released through the parental cell wall. Upon release, they typically aggregate near the vegetative cells that produced them (Fig. 6) and adhere to the substrate using their flagella. Shortly after flagellar loss, they secrete mucus through flagellar pores in the cell wall, forming a small disc–shaped pad that facilitates attachment to other cells or substrates (Figs 2, 6).

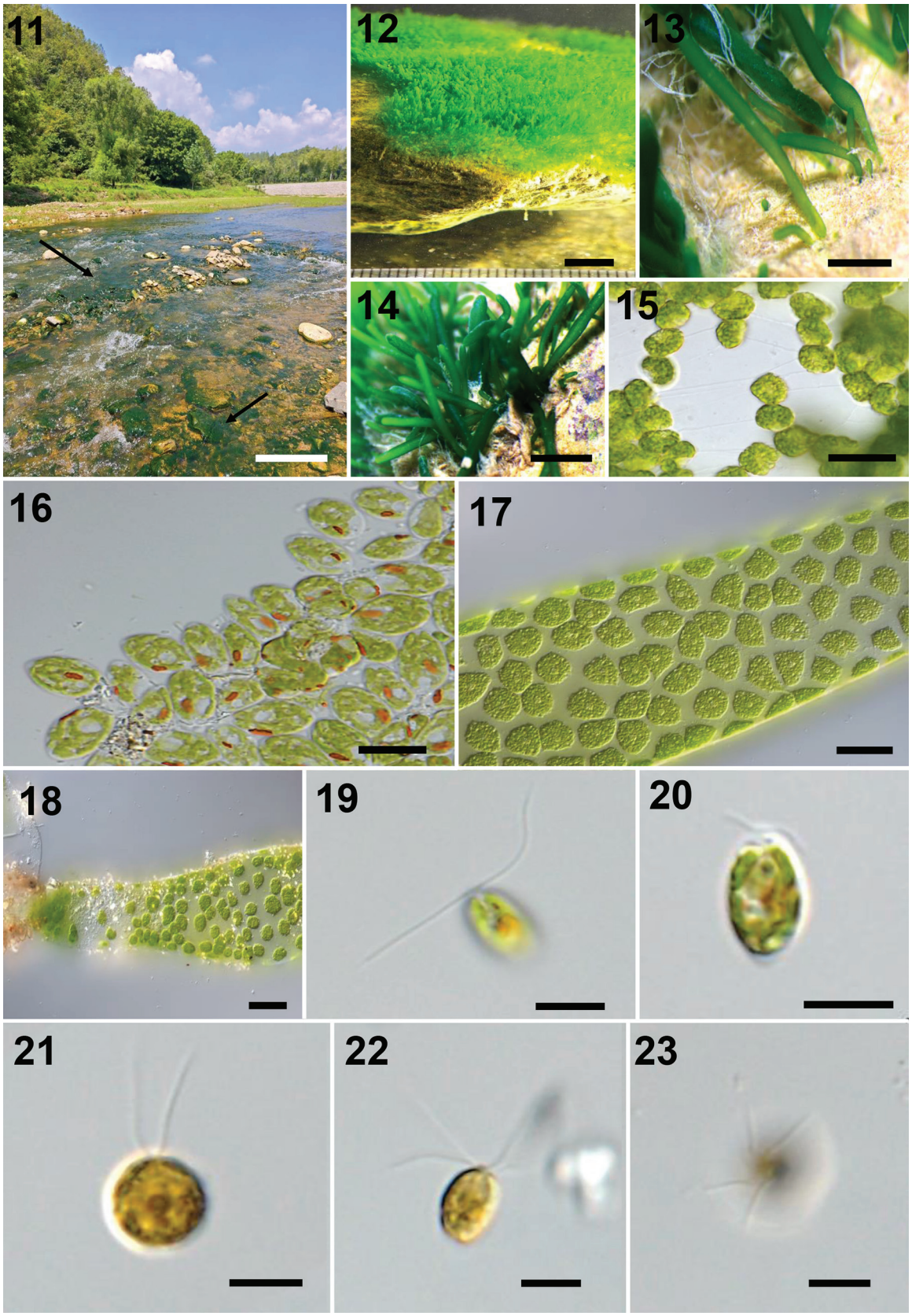
The thalli of the strains MTGZ01 and WHGZ02 are dark green in color and significantly larger (Fig. 12). In their colonial form, individual thalli cluster together, with each thallus base attached to a substrate (Figs 13, 14). The thallus is unbranched and rod–shaped, with a bluntly rounded apex that gradually narrows toward the base. The base is slightly enlarged to facilitate substrate attachment (Fig. 13). The thalli measure 9–15 mm in length, with their width can reaching 0.5–1.2 mm. The entire surface of the thallus is covered by a colorless, transparent cuticle. Immediately beneath the cuticle is a layer of morphologically distinct and externally exposed cells, previously called "protocoenocytes" (Iyengar, 1936). These cells surround a large central cavity filled with liquid (Figs 17, 18). The cells possessing a cytoplasmic



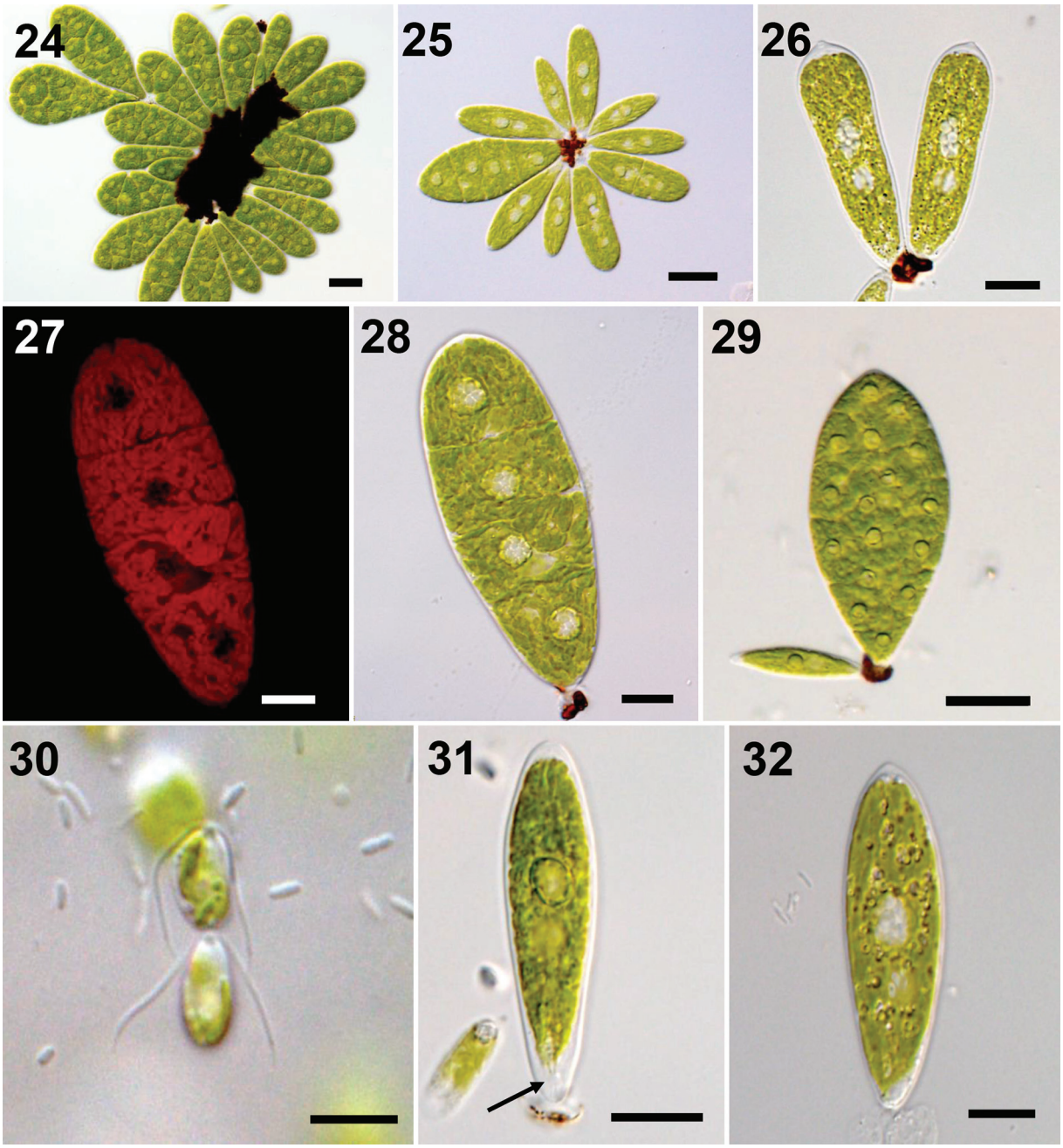
Figs 1–10. Morphology of *Lobocharacium coloradoense* (FACHB–3670). **(1)** Morphology of cell–aggregated colonies. **(2)** Cells attached to other cell. **(3, 4)** Central pyrenoid and chloroplasts with slight surface wrinkles. **(5)** Division of plastids. **(6)** Young cells aggregated after cell division. **(7)** The plastid structure connected by cytoplasmic bridges. **(8)** Sporangium in the germination stage. **(9, 10)** Zoospores, with two equal–length flagella slightly longer than the cell itself. Scale bars 40 µm (1), 20 µm (2), 5 µm (3, 4, 5, 9, 10) and 10 µm (6, 7, 8).

membrane but lack a cell wall. They exhibit slight variations in shape and are interconnected by thin cytoplasmic strands (Fig. 15). In young cells, a centrally positioned, stellate chloroplast is observed, which progressively migrates toward the cell periphery during maturation. As starch grains accumulate, the chloroplast shape becomes difficult to discern; however, a large pyrenoid is consistently present (Fig. 17). A single nucleus is embedded within the chloroplast, and the cytoplasm is often laden with starch grains. The shape and spatial arrangement of the cells vary, with cells being most densely packed at the apex and gradually becoming more loosely arranged toward the base (Figs 17, 18). Due to continuous cell division and mutual compression, the cells appear polygonal in frontal view (20–40 µm in width). In regions with wider intercellular spaces, the cytoplasmic strands connecting cells are more prominent (Figs 15, 18). This species reproduces asexually via zoospore formation and sexually through gametogenesis. Following multiple divisions of vegetative cells, zoospores are released. Zoospores are spindle–shaped, measuring 5.5–6.5 µm in length, with a papilla at the anterior end. They possess an eyespot and two flagella of equal length, each approximately 1.5 times the length of the cell. A stellate chloroplast with a central pyrenoid is present (Figs 19, 21). Additionally, gamete production was observed in this study. Gamete formation is similar to that of zoospores, but the gametes are smaller and have oval or slightly irregular shapes. During the fusion of the presumed zygotes (Stewart et al., 1978), the flagella extend outward in an ‘X’–shaped configuration and gradually shorten until they disappear (Figs 20, 22, 23). We discovered this alga in a freshwater

Fottea, 26(1), 94–106, 2026
doi: 10.5507/fot.2025.018



Figs 11–23. Habitat and morphology of *Characiosiphon rivularis* (MTGZ01 & WHGZ02). **(11)** Habitat of *Cn. rivularis*, with the arrow indicating the sampling site. **(12)** *Cn. rivularis* clings to stones, forming dense clusters. **(13,14)** Morphology of cell–aggregated colonies. **(15)** Slender intercellular connecting filaments. **(16)** Zoospores aggregating shortly after formation. **(17)** Cells loosely arranged in the central region of the thallus. **(18)** The thallus base. **(19)** Zoospores, with two equal–length flagella longer than the cell itself. **(20)** Flagella about to degenerate. **(21–23)** Presumed Zygotes at the fusion stage, with flagella extending outward in an "X" shape. Scale bars 0.5 m (11), 5 cm (12), 0.25 cm (13), 0.5cm (14), 10 µm (15), 40 µm (17, 18) and 5 µm (16, 19, 20, 21, 22, 23).



Figs 24–32. Morphology of *Characiochloris papillata* sp. nov. (FACHB–3671). **(24)** Morphology of cell–aggregated colonies. **(25)** Radially arranged cells with a brown attachment pad at the base of cells. **(26)** Papilla at the apex of the cell. **(27)** Chloroplast with perforated and lamellate structures. **(28, 29)** Cells about to divide. **(30)** Zoospores, with two equal–length flagella longer than the cell itself. **(31)** Degenerated flagella and attachment pad. **(32)** Small vacuoles irregularly distributed in the cell. Scale bars 10 μm (24–29, 31–32) and 5 μm (30).

bay area, growing in a slow–flowing stream. Unlike previous reports in which this species was described as occurring only in small numbers, we observed a massive accumulation that entirely covered the streambed (Fig. 11). A close–up photograph was taken in the laboratory, using stones collected from the location marked (Figs 11,12).

The thallus of FACHB–3671 exhibits a radial growth pattern, expanding outward. A brown attachment pad forms at the base of the cells, functioning as a holdfast to interconnect cells or secure them to substrates (Fig. 24). The size of these attachment pads varies within cultures: some are relatively large and darker in color (Fig. 24), while others appear smaller and are restricted to the cell ends for connection (Fig. 25). Mature vegetative cells are rod–shaped or oval, with bluntly rounded apices. They are widest at the upper or middle part of the cell and gradually taper towards the base. The cell wall at the apex is slightly thickened, forming a small papilla (Fig. 26). The cells measure 15–60 μm in length and 4–17 μm in width. Each cell contains a large central pyrenoid encased by a starch sheath, with a prominent

Table 2. Comparison of morphological features among *Characiochloris papillata* and similar species.

Species (references)	Cell shape (size in µm)	Chloroplast	Pyrenoid	The Widest Position	Contractile vacuoles	stalk	The shape of the distal end of the cell	Zoospore		
								Quantity	Size	Flagellar length
Characiochloris papillata (this study)	Rod–shaped or fusiform, 15–60 µm long, 4–17 µm wide.	Single, parietal, with longitudinal stripes and fissures.	1	Apical or middle	Multiple, irregularly distributed.	stalkless	Blunt–rounded, cell wall thickened, small papillary protrusion	2–32	2–6µm long; 2–4µm wide	Equal length, ~1.5× cell
Characiochloris acuminata (Lee & Bold, 1974)	Fusiform, 60 µm long and 30 µm wide.	Single, parietal, with longitudinal stripes and fissures.	1	Middle or basal	Multiple, irregularly distributed.	stalkless	Acute	2–16	12–19µm long; 4.5–7.7µm wide	Equal length, ~1–1.5× cell
Characiochloris clathrata (Skuja, 1956)	Ellipsoidal or oval, 18–38 µm long and 14–35 µm wide.	Single, parietal, clathrate, with fissures.	2–6	Middle	Two, near the proximal end of the protoplast.	A short stalk.	Bluntly rounded or gradually tapering	4–8	13–20µm long; 6–12µm wide	Equal and shorter, ~0.8–1× cell
Characiochloris characioides (Pascher, 1927)	Fusiform, 20–50 µm long and 5–9 µm wide.	Single, parietal, with longitudinal stripes and fissures.	1	Middle	Multiple, irregularly distributed.	stalkless	Acute	Up to 32	Up to 20µm long	Equal and shorter, ~0.5–0.6× cell
Characiochloris sasae (Nozaki, 1993)	Slender fusiform, up to 40 µm long and up to 16 µm wide.	Single, parietal, with longitudinal stripes and fissures.	1	Middle or basal	Multiple, irregularly distributed.	stalkless	Large, conspicuous papillary blunt protrusions	16–256	10–14µm long	Equal and longer, ~1.2–2.5× cell
Characiochloris sessilis (Pascher, 1927)	Oval or pyriform, 12–24 µm long and 6–16 µm wide.	Single, parietal, with longitudinal stripes and fissures.	1	basal	Multiple, irregularly distributed.	stalkless	Acute	2–4	Not mentioned.	Not mentioned.
Characiochloris apiculata (Korshikov, 1953)	Ellipsoidal or oval, up to 40 µm long and 11–22 µm wide.	Single, parietal, with longitudinal stripes and fissures.	1	Middle	Multiple, irregularly distributed.	A thin and short stalk.	Small papillary protrusions formed by cell–wall thickening	32–64	13–14µm long	Equal, ~2× cell

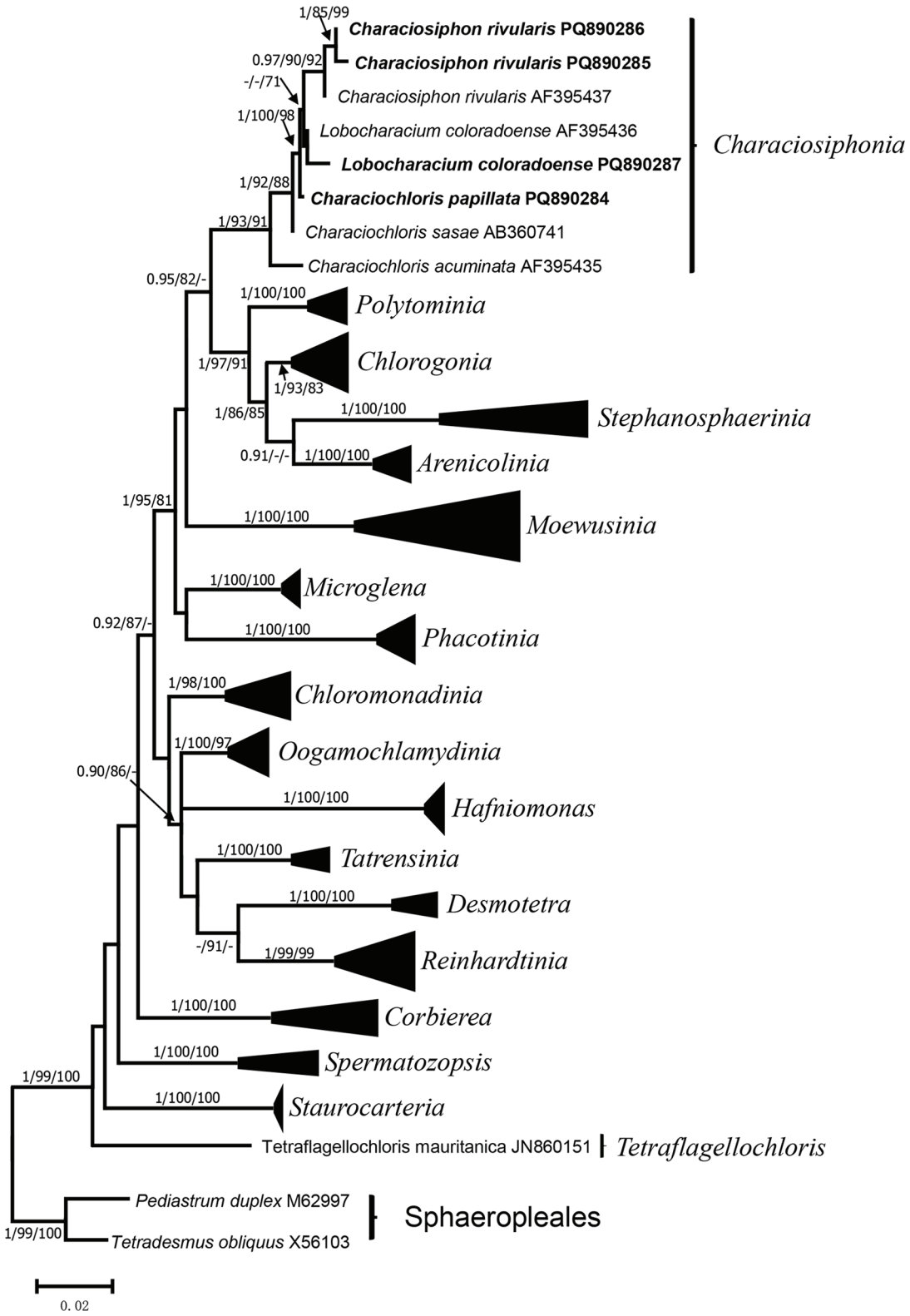


Fig. 33. Molecular phylogeny of the Chlamydomonadales inferred by Bayesian inference, based on 18S rDNA sequences, with two sequences from the Sphaeropleales used as outgroups. Bayesian posterior probabilities (PP) greater than 0.90, Shimodaira–Hasegawa–like approximate likelihood ratio (SH–aLRT) values above 80%, and bootstrap value (BP) exceeding 70% in the maximum likelihood (ML) analysis are displayed on the branches from left to right.

Fottea, 26(1), 94–106, 2026
doi: 10.5507/fot.2025.018

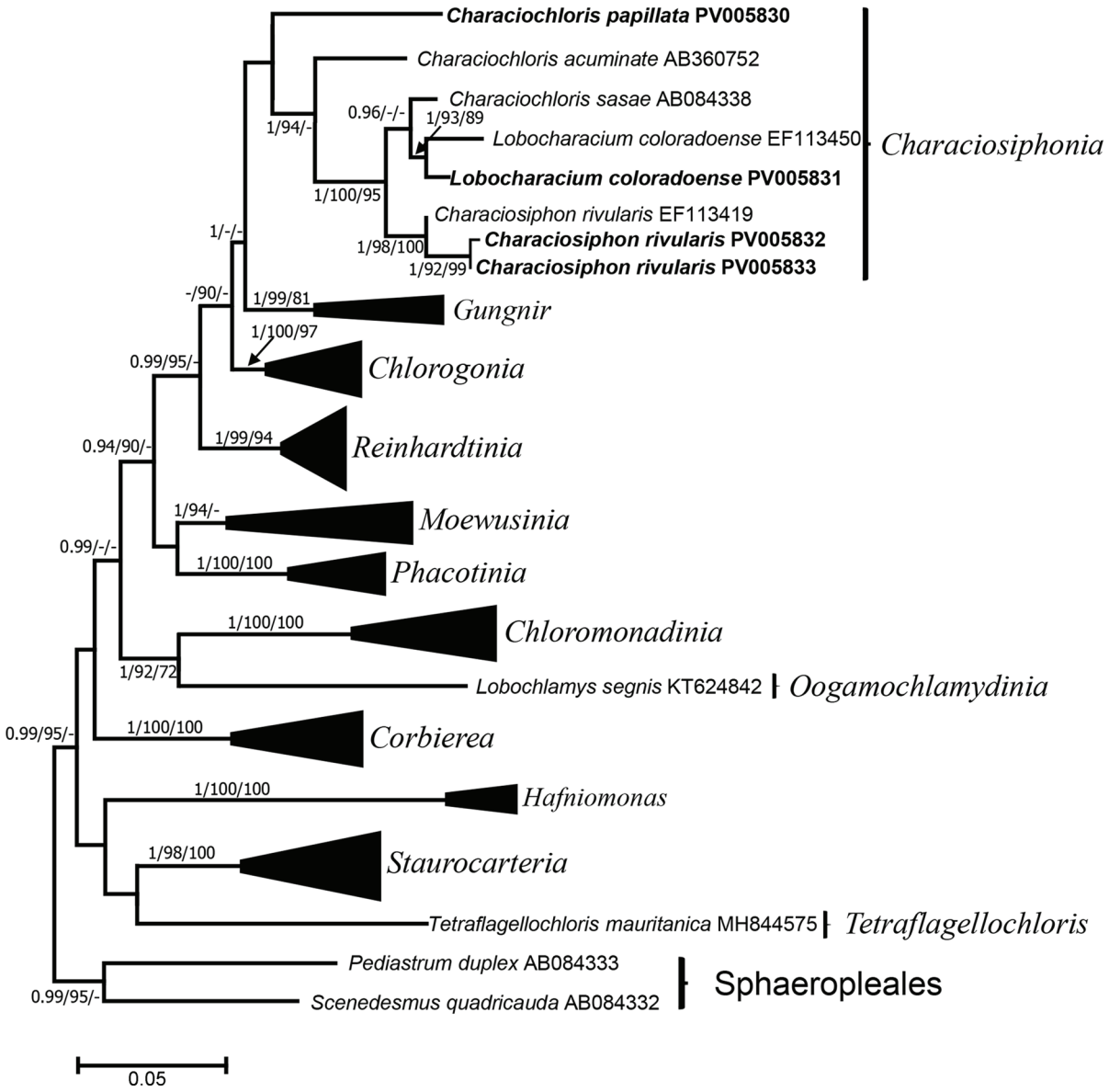


Fig. 34. Molecular phylogeny of the Chlamydomonadales inferred by the maximum likelihood method, based on *rbcL* gene sequences, with two sequences from the Sphaeropleales used as outgroups. Support values are the same as in Fig. 33.

contractile vacuole situated beneath (Fig. 25). At the base of the cell, two degenerated flagella are occasionally faintly visible (Fig. 31). A single chloroplast occupies most of the cell and exhibits distinct longitudinal striations and fissures. The plastid forms layered folds with visible perforations (Figs 27, 28). Additionally, numerous small contractile vacuoles are dispersed throughout the protoplast (Fig. 32). Under laboratory conditions, the vegetative cells typically divide to produce 8, 16, or 32 zoospores (Figs 24, 25, 29). These zoospores measure 2–6 µm in length and 2–4 µm in width. They are elongated and oval–shaped, possessing two equal–length flagella approximately 1.5 times the length of the cell (Fig. 30). Zoospores are released from the parental cell wall and attach to the substrate via their flagella. Following attachment, the flagella degenerate and disappear, allowing the cell to develop into a vegetative cell (Fig. 29). Its main characteristic is the irregularly contractile vacuoles in cells. The comparison with other species in the genus is provided in Table 2.

Molecular phylogenetic analyses

Bayesian and maximum likelihood (ML) analyses were performed using the four strains–FACHB–3670, MTGZ01, WHGZ02, and FACHB–3671. The 18S rDNA phylogenetic analysis showed that the four strains clustered within the *Characiosiphonia* clade fully supported by a PP of 1.0 and a BP of 91 (Fig. 33). The strains MTGZ01 and WHGZ02 showed strong phylogenetic affinity with *Cn. rivularis*, supported by a Bayesian posterior probability of 0.97 and bootstrap value of 92, suggesting they are the same species. This molecular evidence was further corroborated by morphological identification. In the *rbcL* phylogenetic tree (Fig. 34), strain FACHB–3670

clustered with *Lm. coloradoense* with strong statistical support (PP=1.0, BP=89), suggesting they represent the same species.

The phylogenetic analysis based on *rbcL* showed a topology partially similar to that obtained from the 18S rDNA dataset. However, the branching patterns differ in several important aspects. In the 18S rDNA phylogenetic tree (Fig. 33), *Characiochloris papillata* is nested within the *Characiosiphonia* clade and failed to cluster with *Characiochloris acuminata* K.W. Lee *et* H.C. Bold and *Characiochloris sasae* H. Nozaki. They each occupy a separate branch and failed to form a monophyletic lineage. Although the overall *Characiosiphonia* clade is strongly supported (PP = 1.0, BP = 91).

In the *rbcL* phylogenetic tree (Fig. 34), *Cs*. *papillata* at the upper position within the *Characiosiphonia* clade and remains separated from *Cs. sasae* and *Cs. acuminata.* However, in contrast to the 18S rDNA phylogeny–where *Cs. papillata* shows a closer relationship to *Lm. coloradoense*–the *rbcL* tree reveals a different pattern, with *Cs. sasae* clustering together with *Lm. coloradoense*. Although the support for the entire clade including *Cs*. *papillata* is somewhat reduced, the core group excluding this taxon–comprising *Lm. coloradoense* and *Cn. rivularis*–retains strong statistical support (PP = 1.0, BP = 94).

Notably, in both phylogenies, the species was classified under *Characiochloris* (C*s*. *acuminata* and *Cs. sasae*) consistently failed to form a monophyletic lineage. Furthermore, both of the 18S and *rbcL* phylogenetic analyses, strain FACHB–3671 failed to cluster with other species within *Characiochloris*, this indicates that the genus is not a monophyletic taxon.

***Characiochloris papillata* Q.Y.Dai *et* G.X.Liu *sp. nov.* (Figs. 24–32)**

Description: Mature vegetative cells are fusiform or elliptical with obtuse apices, widest at the upper or middle part, and gradually narrowing toward the base. The cell apex is slightly thickened, forming a small papilla. The basal part bears a brown, gelatinous attachment pad, which serves as a holdfast anchoring the cell to substrates. A single chloroplast with longitudinal striations and fissures occupies most of the cell. A central pyrenoid, encased by a starch sheath. Irregularly shaped, small contractile vacuoles are distributed throughout the protoplast. Occasionally, two degenerated flagella are visible at the base of the cell. Asexual reproduction occurs through the release of biflagellate zoospores. The zoospores are elongated and elliptical, equipped with two equal–length flagella approximately 1.5 times the cell length. Upon release, the zoospores attach to substrates via their proximal end. Subsequently, the flagella degenerate and disappear as the zoospores develop into vegetative cells. Mature vegetative cells measure 15–60 µm in length and 4–17 µm in width. Zoospores are 2–6 µm long and 2–4 µm wide. Sexual reproduction has not been observed.

Holotype: Dry specimen number HBI XW–C1 collected by Qingyu Dai on October 10, 2022, and preserved in Freshwater Algae Specimen Station, Institute of Hydrobiology, Chinese Academy of Sciences, Wuhan, Hubei Province, China. Habitat: epilithon, growing on the surface of submerged stones in freshwater. Reference strain: living strain permanently preserved in the Freshwater Algae Culture Collection, Institute of Hydrobiology, Chinese Academy of Sciences, Wuhan, China (FACHB) as FACHB–3671.

Type locality: On stones in a small river in Xuanwei City, Yunnan Province, China. 26.2126°N, 104.1085°E.

Etymology: The species name is derived from the cell apex is slightly thickened, forming a small papilla.

Comments: Based on previously published species descriptions, as listed in Table 2, *Cs. papillata* is most similar to *Cs. acuminata* (Lee & Bold, 1974). However, the two species differ in that the apex of *Cs. papillata* forms a small papilla due to thickening of the cell wall, a structure that absent in *Cs. acuminata*, whose cell apex is acute. In contrast, the apex of *Cs. papillata* is rounded and occasionally narrows. Compared to *Cs. clathrata* (Skuja, 1956), *Cs. papillata* has only one pyrenoid, while *Cs. clathrata* typically contains 2–6 pyrenoids. Moreover, *Cs. clathrata* forms a stalk at the base of the cell, which is absent in *Cs. papillata*. When compared to *Cs. characioides* (Pascher, 1927), the widest part of *Cs. papillata* is located at the mid or apex of the cell, while the widest part of *Cs. characioides* is at the middle of the cell. Additionally, *Cs. characioides* has an acute distal end, which *Cs. papillata* lacks. *Cs. sasae* (Nozaki, 1993) possesses a pronounced papilla occupying about one–third of the cell, whereas the small papilla in *Cs. papillata* is formed by thickening of the cell wall, showing a clear distinction from *Cs. sasae*. In comparison to *Cs. sessilis* (Pascher, 1927) and *Cs. apiculata* (Korshikov, 1953), the widest point of *Cs. papillata* is notably different, and there are differences in the number of zoospores formed as well as the shape of the cell's distal end. Furthermore, *Cs. apiculata* forms a small stalk, which distinguishes it from *Cs. papillata* and *Cs. sessilis*, both of which lack stalks. Therefore, from a morphological standpoint, it can be concluded that *Cs. papillata* is a new species distinct from other species within the genus *Characiochloris*.

Discussion

This study provides a detailed morphological description of four strains. The strain FACHB–3670 was identified as *Lm. coloradoense*, and strains MTGZ01 and WHGZ02 were identified as *Cn. rivularis*. The phylogenetic results indicate that *Lobocharacium*, *Characiosiphon*, and *Characiochloris* form a clade with robust support. The strain FACHB–3671 clusters separately from other species

Fottea, 26(1), 94–106, 2026
doi: 10.5507/fot.2025.018

within *Characiochloris*, suggesting that the genus is not monophyletic. Observations of strain FACHB–3671 has a morphological similarity to *Characium* (Kützing, 1849). However, unlike the species of the genus *Characium*, this strain has some irregularly contractile vacuoles within cells– an important characteristic feature of the genus *Characiochloris*. Pascher (1927) established *Characiochloris* with *Characiochloris characioides* Pascher as the type species. In the description of *Characiochloris* in 1927, the cells were noted to resemble those of *Characium* but lacked a stalk, attaching instead by means of a small gelatinous pad that may be encrusted with iron deposits. The cell wall is smooth, and the cell membrane is typically very thin, only rarely surrounded by a delicate gelatinous envelope. A single chloroplast occupies most of the cell and shows distinct longitudinal striations or fissures of varying prominence. When this genus was established, only two species, *Cs. characioides* and *Cs. sessilis*, were described and assigned to it. With the accumulation of samples, more species have been included in this genus. However, as of now, the NCBI database contains molecular data for only two species, *Cs. acuminata* and *Cs. sasae*, both of which are used in this study. *Cs. acuminata* was first described based on its contractile vacuoles, which are located in the cells. Compared to *Cs. characioides*, *Cs. acuminata* has smaller vegetative cells, and its flagella are longer than the length of the zoospores. (Lee & Bold, 1974). *Cs. sasae,* described by Nozaki (1993), was identified by its prominent anterior papilla, which is approximately one–third the length of the cell, and possessing several irregularly contractile vacuoles within the cytoplasm. These observations suggest that the irregular contractile vacuoles can be used a character for recognizing members of the genus *Characiochloris*. In our observations of strain FACHB–3671, we found that aside from the presence of several irregular contractile vacuoles in the vegetative cells, no recognizable gelatinous matrix was observed around the cells, even in older cultures. Notably, Nozaki (1993) also reported the absence of a gelatinous matrix in his description of *Characiochloris sasae*. With respect to chloroplast morphology, strain FACHB–3671 clearly exhibits longitudinal striations or fissures, whereas chloroplasts in most *Characium* species are lamellate and lack such longitudinal structures. These diagnostic characters indicate that the morphology of strain FACHB–3671 corresponds closely to published descriptions of *Characiochloris*. Moreover, the limited availability of molecular data for *Characiochloris* has also made it difficult to determine its taxonomic position. The molecular data for *Cs. acuminata* were first provided by Buchheim *et al.* (2002); however, in that study, this species was not included in any phylogenetic analysis. Later, Nakada *et al*. (2008) published a study that included the molecular data of *Lm. coloradoense*, *Cn. rivularis*, *Cs. acuminata*, and *Cs. sasae*. Their analysis showed that these four taxa formed a clade, which they referred to as the "*Lobocharacium* lineage". Notably, *Cs. acuminata* and *Cs. sasae* failed to cluster, and *Lm. coloradoense* clustered with *Cs. sasae*, supporting *Characiochloris* is not monophyletic. In a follow–up study published the same year, Nakada *et al*. (2008) excluded *Cs. sasae* from the analysis, which resulted in a clade comprising *Lm. coloradoense, Cn. rivularis, and Cs. acuminata*–a lineage now recognized as the *Characiosiphonia* clade. The phylogenetic analyses in our study, which excluded the newly isolated strain FACHB–3671, are consistent with the results of Nakada *et al*. (2008) and further support that *Characiochloris* is not monophyletic. Considering these diagnostic traits, the morphology of strain FACHB–3671 is more consistent with previously published descriptions of *Characiochloris*. When taken together with its phylogenetic position, this evidence supports recognizing the strain as a new species, which we described as *Characiochloris papillata* sp. nov. Therefore, we tentatively place strain FACHB–3671 within *Characiochloris*, while noting that further taxonomic revision will be necessary to more accurately reflect the phylogenetic relationships within this genus.

Pascher (1927) thought it cannot be ruled out that some of the *Characium* species described so far, which have been little studied overall, may actually belong to *Characichloris*. In light of our findings, we agree with this statement; it is clear that the current generic circumscription of *Characiochloris* needs re–evaluation. Future taxonomic work should include sequencing and broader sampling of the type species and closely related taxa.
Compared with *Characiochloris,* both *Lobocharacium* and *Characiosiphon* have only one species. *Cn. rivularis* has been recorded in several parts of the world (Agarkar, 1953; Bhandari, 1955; Iyengar, 1936; Sharma, 1958.). However, there is no other one described within the genus. And *Lobocharacium* has only been reported by Kugrens *et al.* (2000) and this study. Interestingly, although *Cn. rivularis* has been considered a rare taxon (Sarma & Keshri, 1992), we discovered an exceptionally abundant population of *Cn. rivularis* in a stream, where it covered the streambed. This extensive and nearly monospecific growth provides novel insights into the ecological distribution and potential adaptability of this species.

In laboratory culture, we also observed that the cell size of *Lm. coloradoense* was significantly smaller than that described by Kugrens *et al.* (2000). This difference might be caused by changes in environmental conditions or habitat. More research is needed to understand what causes such variation in cell size.

Phylogenetic analyses indicate that *Characiochloris*, *Lobocharacium*, and *Characiosiphon* clustered to form the *Characiosiphonia* clade. However, due to the limited number of species and the scarcity of molecular data within this clade, it remains difficult to further resolve the phylogenetic relationships among its members and to clearly define its taxonomic boundaries. In future studies, we aim to collect more species and molecular data within this clade, and to conduct genome sequencing and analysis of the existing strains. These efforts will help us gain deeper insights into the clade.

Acknowledgements

This research was funded by the National Natural Science Foundation of China (Grant No. 32270226) and Science & Technology Fundamental Resources Investigation Program of China (Grant No. 2023FY101305). This study complies with all scientific and ethical standards in biological research. No special permits were required, and the work does not involve protected species, regulated genetic resources, or any form of plagiarism.

References

Agarkar, M. S. (1953). Note on *Characiosiphon rivularis* Iyengar from Gwalior. *Current Science, 22*(8), 245–246.

Bhandari, M. M. (1955). Occurrence of *Characiosiphon rivularis* Iyengar. *Current Science, 24*(1), 16–17.

Bischoff, H. W., & Bold, H. C. (1963). *Phycological studies IV: Some soil algae from Enchanted Rock and related algal species* (University of Texas Publication No. 6318). University of Texas.

Bourrelly, P. (1959). Initiation pratique à la systématique des algues d'eau douce. VII. Tetrasporales (Complément). *Bulletin de la Société de Microscopie Appliquée*, *9*, 51–68.

Buchheim, M. A., & Buchheim, J. A. (2000). *Characiochloris* and *Characiosiphon* form a sister group to the *Dunaliella* lineage. *Journal of Phycology, 36*(1), 1–8. https://doi.org/10.1046/j.1529-8817.2000.99001.x

Buchheim, M. A., Buchheim, J. A., Carlson, T., & Kugrens, P. (2002). Phylogeny of *Lobocharacium* (Chlorophyceae) and allies: A study of 18S and 26S rDNA data. *Journal of Phycology, 38*(2), 376–383. https://doi.org/10.1046/j.1529-8817.2002.01145.x

Edgar, R. C. (2004). MUSCLE: Multiple sequence alignment with high accuracy and high throughput. *Nucleic Acids Research, 32*(5), 1792–1797. https://doi.org/10.1093/nar/gkh340

Ettl, H., & Gärtner, G. (1988). Eine einfache Methode zur Darstellung der Struktur der Stärkehüllen von Pyrenoiden bei Grünalgen (Chlorophyta). *Archiv für Protistenkunde, 135*(1–4), 179–181. https://doi.org/10.1016/S0003-9365(88)80065-4

Fott, B. (1959). *Algenkunde*. VEB Gustav Fischer.

Fott, B. (1972). Chlorophyceae, Tetrasporales. In G. Huber-Pestalozzi (Ed.), *Das Phytoplankton des Süsswassers* (Vol. 16, pp. 94–95). Schweizerbart.

Fott, B. (1972). Taxonomische Übertragungen und Namensänderungen unter den Algen. V. Tetrasporales. *Preslia, 44,* 193–207.

Guindon, S., Dufayard, J. F., Lefort, V., Anisimova, M., Hordijk, W., & Gascuel, O. (2010). New algorithms and methods to estimate maximum–likelihood phylogenies: Assessing the performance of PhyML 3.0. *Systematic Biology, 59*(3), 307–321. https://doi.org/10.1093/sysbio/syq010

Iyengar, M. O. P. (1936). *Characiosiphon,* a new member of the Chlorophyceae: Preliminary note. *Journal of the Indian Botanical Society, 15,* 313–318.

Iyengar, M. O. P. (1960). Some interesting green algae. In P. Kachroo (Ed.), *Proceedings of the Symposium on Algology* (pp. 380–406). Indian Council of Agricultural Research.

Iyengar, M. O. P. (1975). Contributions to our knowledge of South Indian algae – VIII. *Proceedings of the Indian National Science Academy, Section B, 81*(1), 29–60.

Kalyaanamoorthy, S., Minh, B. Q., Wong, T. K., von Haeseler, A., & Jermiin, L. S. (2017). ModelFinder: Fast model selection for accurate phylogenetic estimates. *Nature Methods, 14*(6), 587–589. https://doi.org/10.1038/nmeth.4285

Katoh, K., & Standley, D. M. (2013). MAFFT multiple sequence alignment software version 7: Improvements in performance and usability. *Molecular Biology and Evolution, 30*(4), 772–780. https://doi.org/10.1093/molbev/mst010

Korshikov, A. A. (1953). *Viznachnik prisnovodnykh vodorostei Ukrains'koi RSR. Protococcineae*. Akademiia Nauk Ukrains'koi RSR.

Kugrens, P., Clay, B. L., & Aguiar, R. (2000). Ultrastructure of *Lobocharacium coloradoense,* gen. et sp. nov. (Chlorophyta, Characiosiphonaceae), an unusual coenocyte from Colorado. *Journal of Phycology, 36*(2), 421–432. https://doi.org/10.1046/j.1529-8817.2000.99089.x

Kumar, S., Stecher, G., & Tamura, K. (2016). MEGA7: Molecular evolutionary genetics analysis version 7.0 for bigger datasets. *Molecular Biology and Evolution, 33*(7), 1870–1874. https://doi.org/10.1093/molbev/msw054

Kützing, F. T. (1849). *Species algarum*. F. A. Brockhaus.

Lee, K. W., & Bold, H. C. (1974). *Phycological studies XII: Characium and some Characium-like algae* (University of Texas Publication No. 7413). University of Texas.

Mahajan, S. K. (2008). A new report of *Characiosiphon* from West Nimar District of Madhya Pradesh. *Environment Conservation Journal, 9*(3), 35–36. https://doi.org/10.36953/ECJ.2008.090307

Minh, B. Q., Schmidt, H. A., Chernomor, O., Schrempf, D., Woodhams, M. D., von Haeseler, A., & Lanfear, R. (2020). IQ–TREE 2: New models and efficient methods for phylogenetic inference in the genomic era. *Molecular Biology and Evolution, 37*(5), 1530–1534. https://doi.org/10.1093/molbev/msaa015

Nakada, T., Misawa, K., & Nozaki, H. (2008). Molecular systematics of Volvocales (Chlorophyceae, Chlorophyta) based on exhaustive 18S rRNA phylogenetic analyses. *Molecular Phylogenetics and Evolution, 48*(1), 281–291. https://doi.org/10.1016/j.ympev.2008.03.016

Nakada, T., Nozaki, H., & Pröschold, T. (2008). Molecular phylogeny, ultrastructure, and taxonomic revision of *Chlorogonium* (Chlorophyta): Emendation of *Chlorogonium* and description of *Gungnir* gen. nov. and *Rusalka* gen. nov. *Journal of Phycology, 44*(3), 751–760. https://doi.org/10.1111/j.1529-8817.2008.00525.x

Nakazawa, A., Yamada, T., & Nozaki, H. (2004). Taxonomic study of *Asterococcus* (Chlorophyceae) based on comparative morphology and rbcL gene sequences. *Phycologia, 43*(6), 711–721. https://doi.org/10.2216/i0031-8884-43-6-711.1

Nozaki, H. (1993). Morphology, reproduction and taxonomy of *Characiochloris sasae* sp. nov. (Chlorophyta) from Japan. *Phycologia, 32*(2), 129–135. https://doi.org/10.2216/i0031-8884-32-2-129.1

Nozaki, H., Itoh, M., Sano, R., Uchida, H., Watanabe, M. M., & Kuroiwa, T. (1995). Phylogenetic relationships within the colonial Volvocales (Chlorophyta) inferred from rbcL gene sequence data. *Journal of Phycology, 31,* 970–979. https://doi.org/10.1111/j.0022-3646.1995.00970.x

Pascher, A. (1927). *Die Süsswasser-Flora Deutschlands, Österreichs und der Schweiz. Vol. 4: Volvocales (Phytomonadinae)*. Fischer.

Proshkina–Lavrenko, A. (1941). Novye vidy roda *Characiochloris* Pasch. *Botanicheskie Materialy Otdela Sporvykh Rastenii Botanicheskogo Instituta Akademii Nauk SSSR, 5,* 49–60.

Fottea, 26(1), 94–106, 2026
doi: 10.5507/fot.2025.018

Ronquist, F., Teslenko, M., van der Mark, P., Ayres, D. L., Darling, A., Höhna, S., & Huelsenbeck, J. P. (2012). MrBayes 3.2: Efficient Bayesian phylogenetic inference and model choice across a large model space. *Systematic Biology, 61*(3), 539–542. https://doi.org/10.1093/sysbio/sys029

Sarma, P., & Kesri, J. P. (1992). The genus *Characiosiphon* Iyeng. (Chlorococcales) in Eastern India with a note on the genus. *Bangladesh Journal of Botany, 21*(1), 39–42.

Sharma, R. (1958). Asexual reproduction in *Characiosiphon rivularis* Iyengar. *Current Science, 27*(2), 500–501.

Skuja, H. (1948). *Taxonomie des Phytoplanktons einiger Seen in Uppland, Schweden. Symbolae Botanicae Upsalienses, 9,* 1–399.

Skuja, H. (1956). *Taxonomische und biologische Studien über das Phytoplankton schwedischer Binnengewässer. Nova Acta Regiae Societatis Scientiarum Upsaliensis, Series IV, 16*(3), 1–404.

Stewart, J. K., Stewart, J. R., & Bold, H. C. (1978). The morphology and life history of *Characiosiphon rivularis* Iyengar (Chlorophyta: Characiosiphonaceae): A light and electron–microscopic study. *Archiv für Protistenkunde, 120*(3), 312–340. https://doi.org/10.1016/S0003-9365(78)80007-4

Tamura, K., Stecher, G., & Kumar, S. (2021). MEGA11: Molecular evolutionary genetics analysis version 11. *Molecular Biology and Evolution, 38*(7), 3022–3027. https://doi.org/10.1093/molbev/msab120